

Synthesis, characterization and adsorption behavior of Mo(VI) and W(VI) ions on titanium dioxide nanoparticles containing anatase modification

Polina A. Demina · Alexey N. Kuz'michev · Andrei M. Tsybinsky ·
Lubov N. Obolenskaya · Galina M. Kuz'micheva · Elena N. Domoroshchina ·
Elena V. Savinkina

Received: 25 June 2013 / Accepted: 28 October 2013 / Published online: 13 November 2013
© The Author(s) 2013. This article is published with open access at Springerlink.com

Abstract Adsorption of Mo(VI) and W(VI) ions from water with nanosized anatase has been studied. This process depends on sorption conditions (temperature, contact duration, etc.) and sample characteristics (composition, specific surface area, coherent scattering regions, etc.). Maximal recovery efficiency for Mo(VI) and W(VI) was achieved with the use of the samples of commercial Hombifine N ($R_{\text{Mo}} = 99.90\%$) and Degussa P25 ($R_{\text{Mo}} = 99.99\%$, $R_{\text{W}} = 99.75\%$) and nanosized anatase modified with H_2O_2 ($R_{\text{Mo,W}} = 99.75\%$) under optimal conditions of sorption.

Keywords Nanosized titania · Anatase · Adsorption · Water purification

Introduction

The removal of heavy metals from wastewaters is a matter of paramount importance due to the fact that their high toxicity causes major environmental pollution problems. One of the most efficient, applicable and low cost methods for the removal of toxic metals from aqueous solutions is their adsorption on an inorganic adsorbent. Nanosized titanium dioxide attracts interest due to high

speed of As(III) and As(V) (Dadachov 2006a, b; Meng et al. 2003), As(V) (Valencia-Trejo et al. 2010; Deedar et al. 2009; Xiao et al. 2007), U(VI) (Dadachov 2006a, b), Bi(V) (Kuzmicheva et al. 2012), Cu(II) (Georgaka and Spanos 2010), V(V) (Tella et al. 2010), Cu(II) and Mn(II) (Bleam and McBride 1986), Cd(II) (Gao et al. 2004) extracting from aqueous solutions. To achieve high efficiency of adsorption, it is important to understand the effect of the solution parameters and characteristics of adsorbents. The purpose of the project is to study adsorption properties of samples with nano-anatase prepared via a sulfate technique for extraction of Mo(VI) and W(VI) from model water systems. Adsorption of Mo(VI) and W(VI) with titanium dioxide nanoparticles has not been previously reported.

Experimental

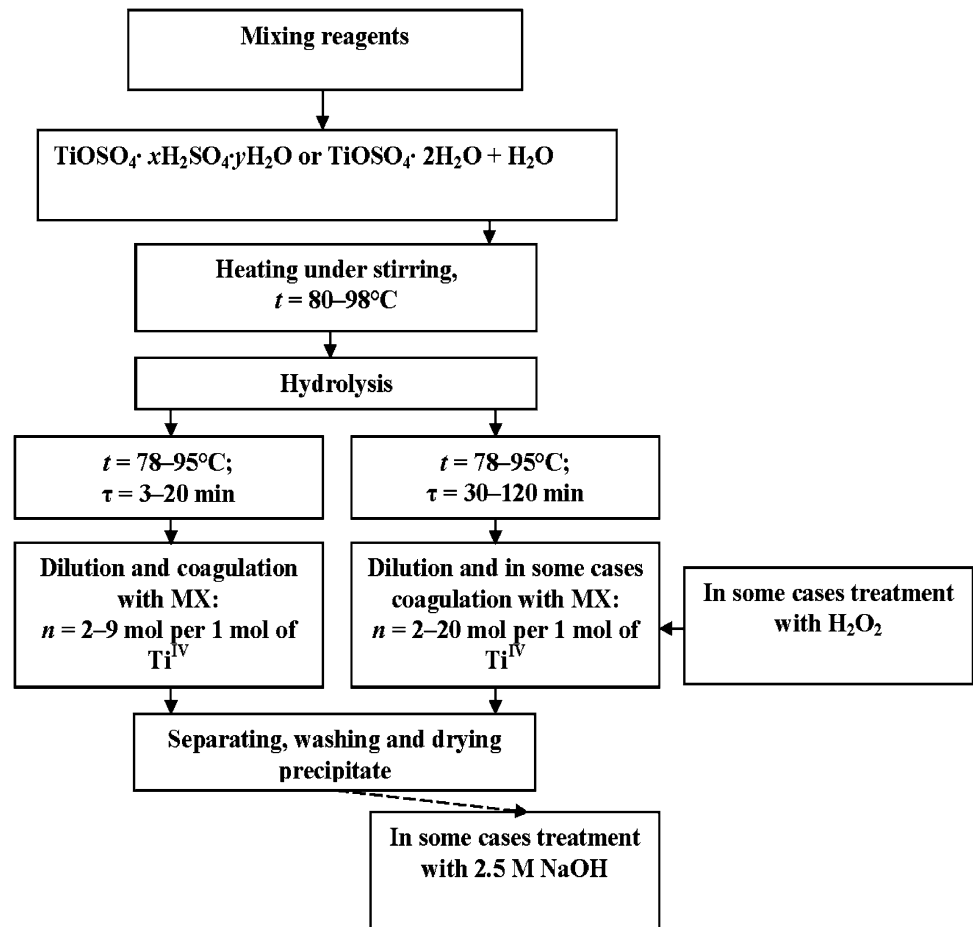
Synthesis

Several types of titania nanoparticles were used in this study. Samples with anatase were prepared using the well-known sulfate method (Kuzmicheva et al. 2010; Savinkina et al. 2011a, b), the main advantages of which is a low temperature of synthesis (not higher than 98 °C) and the possibility of the formation of compounds with the required composition and morphology. The hydrolysis of solvated titanyl sulfate (Aldrich) was performed under mild conditions ($t < 98\text{ °C}$, $\tau = 5\text{--}30\text{ min}$). Various conditions of samples preparation were used (with or without solution stirring, presence or absence of hydrochloric acid, and, in certain instances, treatment with NaOH). The samples were washed with distilled water and acetone, dried and isolated from transparent solutions.

P. A. Demina · A. M. Tsybinsky · L. N. Obolenskaya ·
G. M. Kuz'micheva · E. N. Domoroshchina (✉) ·
E. V. Savinkina
Lomonosov University of Fine Chemical Technology,
119571 Moscow, Russia
e-mail: elena7820@gmail.com

A. N. Kuz'michev
Bonifatius College, Burg. Fockema Andreaelaan 7,
3582 Utrecht, The Netherlands

Fig. 1 Scheme of the synthesis



Anatase was modified with H_2O_2 by treatment of the reaction mixture with hydrogen peroxide while synthesizing titanium dioxide from titanyl sulfate by the earlier reported technique for preparing nanosize anatase (Savinkina et al. 2011a, b). The resulting yellow powders were >20 times washed with water, then with aqueous solution of Na_2SO_3 (to remove uncoordinated H_2O_2 molecules) and finally with acetone (to dry the samples) (Fig. 1).

Commercial Hombifine N and Hombikat UV100 with nanometer-scale anatase and Aeroxide Degussa (Evonik) P25 with the phase composition of ~85 % anatase and ~15 % rutile were also used in this study.

For modifying with H_2O_2 , Hombikat UV100 powder (0.25 g) was dispersed in 50 ml of 10 M solution of H_2O_2 ($\text{TiO}_2:\text{H}_2\text{O}_2 = 1:160$), stirred for 40 min with a magnetic stirrer (30 mm rod) at room temperature, filtered off, washed with water (3–6 times) and acetone (once), dried at room temperature and ground.

X-ray study

All X-ray diffraction (XRD) patterns were recorded with sample rotation on an HZG-4 (Ni filter) diffractometer:

$\text{CuK}\alpha$ radiation in the diffracted beam, stepwise mode (counting time 10 s, a step of 0.02° , 2θ 2° – 50° or 80°). Qualitative XRD phase analyses were carried out using JCPDS PDF-2 and literature data. The coherent scattering region size L (Å) was evaluated using the Scherrer formula:

$$L = 0.9\lambda/\beta \cos \theta, \quad (1)$$

where β is the measured diffraction peak width at half height ($2\theta \sim 25^\circ$).

The sizes of nanoparticles N (nm) were calculated from the results of the small angle X-ray scattering (SAXS) diffractometer, $\text{CuK}\alpha$ (Svergun 1992).

Scanning electron microscopy (SEM)

The microstructures of samples were examined by scanning electron microscopy (SEM) on a JEOL JSM-7500F field-emission scanning electron microscope. Micro- and nanostructures were examined using low-energy back-scattered electron imaging, which insured a resolution of 1.4 nm at 1 kV and 1.0 nm at 20 kV. We also used gentle beam mode, intended to ensure high resolution at a low accelerating voltage.

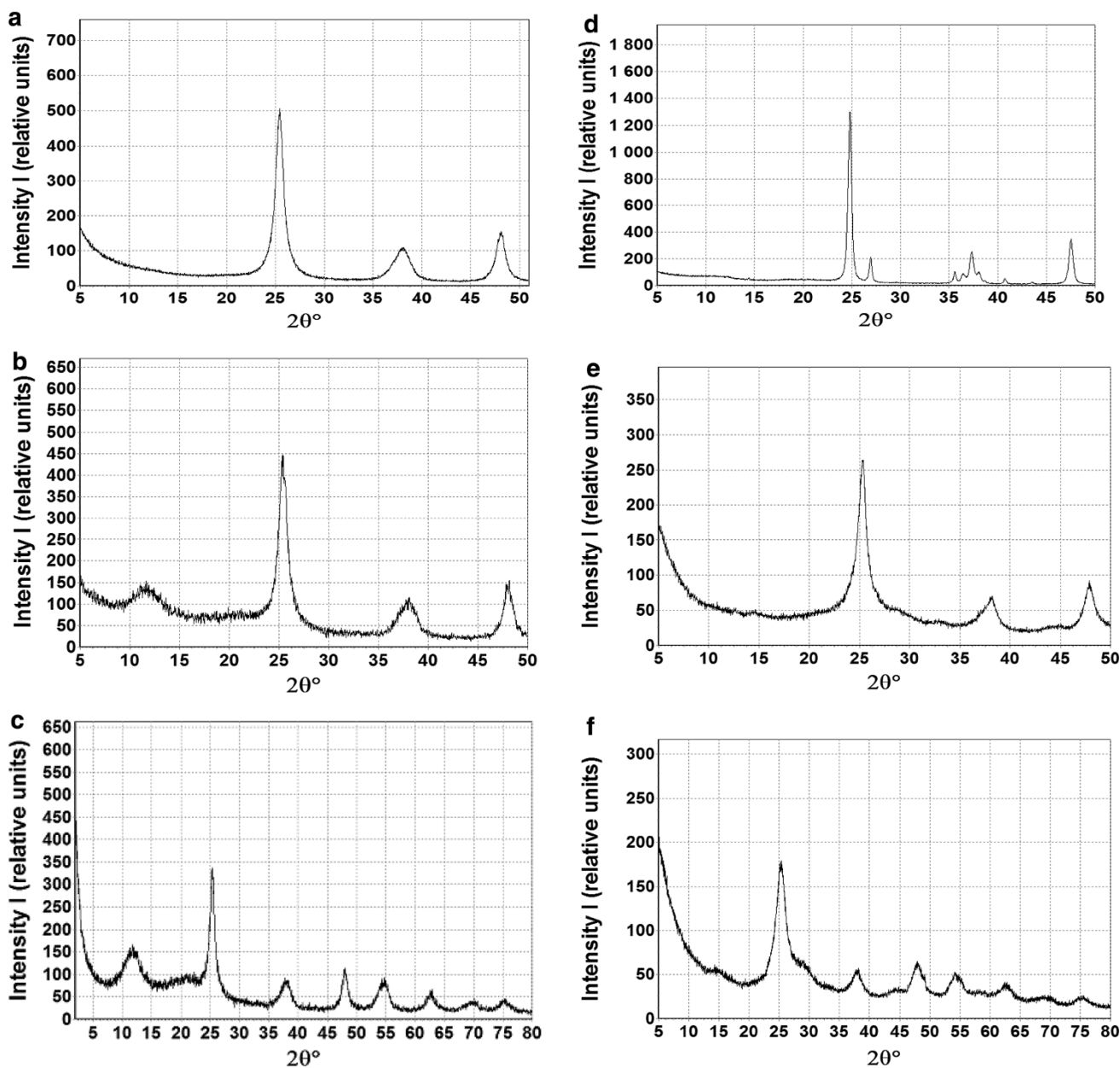


Fig. 2 Plot of the XRD patterns of nanoparticle-sized samples: Hombifine N (a), Hombikat UV100 (b), Hombikat UV100 modified with H₂O₂ (c), Degussa P25 (d), anatase (e), anatase modified with H₂O₂ (f)

Brunauer–Emmett–Teller (BET) method

The appearance and availability of high quality gas analyze sorption data onto the anatase powders using a Micromeritics ASAP 2020 apparatus allowed us to determine the texture characteristics (S m²/g, the free specific surface area; V_N and V_U cm³/g, nano- and ultranopore volumes, correspondingly; N nm, the nanoparticles sizes) of materials and, as a result, to estimate the sizes of particles on whose surfaces adsorption occurs, using the formula (Gregg and Sing 1982; Dzis’ko et al. 1978):

$$N = [K_p / (\rho S)] \times 10^9, \tag{2}$$

where N is the average size of the particles; K_p is the shape factor of the particles ($K_p = 6$ for cubes and spheres). The shape of particles could be revealed from the form of the obtained adsorption isotherms (Obolenskaya et al. 2012; Zhilkina et al. 2013), ρ is the density of the material ($\rho = 3.84$ g/cm³); and S is the specific surface area of the material. The specific surface area of the investigated samples was determined by the Brunauer–Emmett–Teller (S_{BET} , m²/g) (Brunauer et al.

1938) and comparative (S_C , m^2/g) (Zagrafskaya et al. 1975) methods.

Adsorption experiments

Adsorption ability of the samples was studied at pH 0.35 with the use of the standard mixtures ICP-MS-68A-A (High-Purity Standards, USA) containing 1 ppm of analytes (C_i). The Mo(VI) and W(VI) concentration in the solutions after the sorption (C_f) was determined by inductively coupled plasma mass spectrometry (Agilent 7500c, Perkin Elmer ELAN DRC-E, USA). The degree of sorption was evaluated as

$$R = (1 - C_f/C_i) \times 100 \%, \quad (3)$$

where C_f and C_i (the standard deviation was $\pm 2\%$) are final and initial concentrations of analytes, respectively.

Results and discussions

XRD results (Fig. 2) showed that Hombifine N (Fig. 2a), Hombikat UV100 (Fig. 2b) and the most representative samples (Fig. 2e, f) consist of anatase. Degussa P25 (Fig. 2d) contained a significant amount of rutile in addition to the anatase phase.

This is consistent with the literature data that the latter sample with anatase (Fig. 1e) contained, in addition to anatase, small amounts of β -TiO₂ ($2\theta \sim 15^\circ$, $\sim 28^\circ$, $\sim 45^\circ$; JCPDS No. 46-1238). Hombikat UV100 (Fig. 1b) differs from Hombifine N (Fig. 1a) by the presence of hydrous amorphous TiO₂ with the general formula TiO_{2-x}(OH)_{2x} \times yH₂O ($2\theta \sim 12^\circ$).

The characteristics of samples are given in Table 1. Particle diameters for all the samples (N , nm) were taken from SEM photos (N_{SEM}) and calculated from the surface areas determined by the comparative method (S_{CM}). These values for Hombifine N, Hombikat UV100 and Degussa P25 were similar. For very small nanoparticles (anatase and anatase modified with H₂O₂), the particle sizes determined from the BET surface area were somewhat larger than the primary grain sizes and similar to secondary ones (N_{SAXS}) estimated from the small angle X-ray scattering. This difference may be partly attributable to aggregation of individual crystallites, which would reduce the surface area available for N₂ adsorption and, in turn, yield surface area measurements corresponding to larger grain sizes.

SEM images (Kuzmicheva et al. 2010; Savinkina et al. 2011a, b) (in particular, of anatase) (Fig. 3) show agglomeration of primary nanoparticles into the secondary microparticles; the phenomenon is generally observed in nanoparticles synthesis.

Table 1 Characteristics of samples

Symbol	Sample	Value
L (Å)	Hombifine N	83 (4)
	Hombikat UV100	80 (4)
	Degussa P25 ^a	250 (10)
	Anatase	84 (4)
	Anatase modified with H ₂ O ₂ ^b	40 (2)
	Hombikat UV100 modified with H ₂ O ₂ ^b	97 (5)
$N_{SEM,CM}/N_{SAXS}$ (nm)	Hombifine N	12/ $\sim 3 \div 20^a$
	Hombikat UV100	12/ $\sim 3 \div 20^c$
	Degussa P25	28/24
	Anatase	30/10 \div 20 (primary), 30 \div 45 (secondary)
S_{BET}/S_C (m ² /g)	Hombifine N	313 (3)/116
	Hombikat UV100	314/123
	Degussa P25	53.1/54.3
	Anatase	36.5 (4)/16.5
V_U/V_N (cm ³ /g)	Hombifine N	0.083/0.343
	Hombikat UV100	0.082/0.344
	Degussa P25	0.016/0.163
	Anatase	0.013/0.084

^a Data for anatase

^b Characteristics of modified and non-modified samples differ by the coherent scattering region size L only

^c Polydispersity system

The difference between the particle sizes N (nm) and the coherent scattering region size L (Å), that is assumed to be the crystallite size of all the samples (in particular for anatase and anatase modified with H₂O₂) except Degussa P25, is associated with amorphous shells on crystallites.

We have examined adsorption ability of the samples. It was found that the sorption degree (R , %) depends on the sorption conditions. The R value increases with the increase in the sorption duration (T_S) (Fig. 4), the sample weight (m) (Fig. 5) and the use of the membrane filter with 0.45 μ m pores (Fig. 6).

It can be seen that the amount of Mo(VI) and W(VI) ions adsorbed by the TiO₂ nanoparticles from aqueous solutions first decreases and then increases with increasing the temperature from 4–10 to 10–85 $^\circ$ C, respectively, using both filtration through a membrane filter and centrifugation; the latter method allows to decrease duration of residue removal (Fig. 7).

This behavior suggests exothermic nature of the process (in range of 4–10 $^\circ$ C) which can be caused by physical modification of the adsorbents. Surfaces of metal oxides usually have positive charge at low pH (our case: pH 0.35, $i = 0.43(1)$, i -ionic strength). Mo(VI) and W(VI) ions in hydrated associates of different compositions probably have

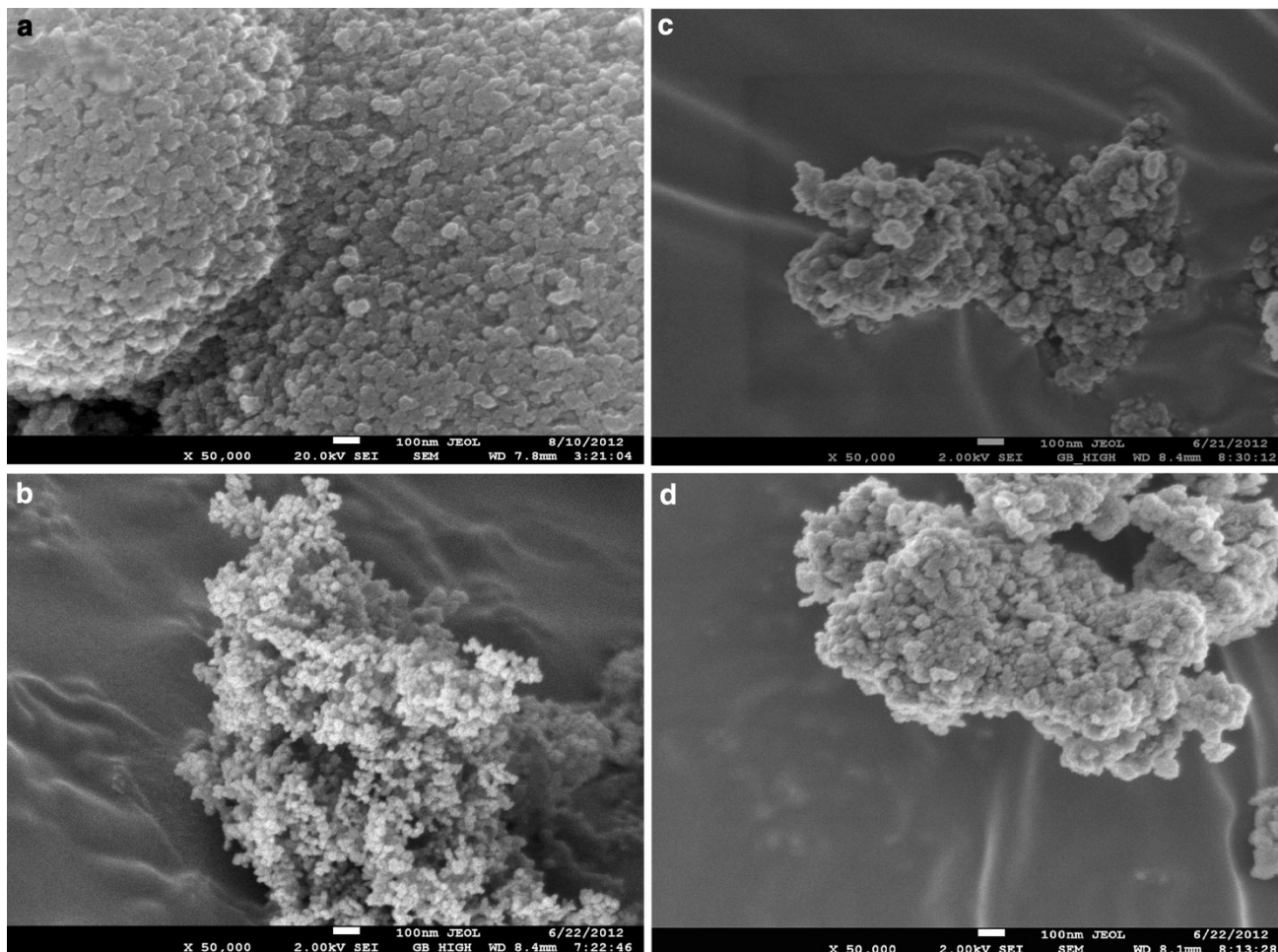


Fig. 3 SEM image of anatase (Fig. 2c) (a), Degussa P25 (Fig. 2b) (b), Hombifine N (Fig. 2a) (c), Hombikat UV100 (Fig. 2b) (d)

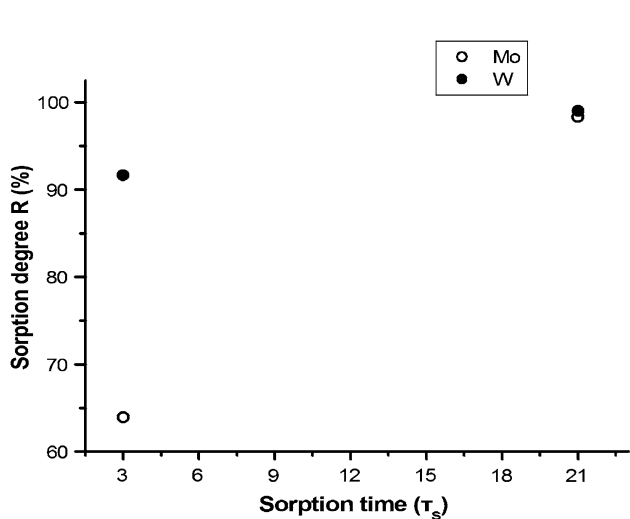


Fig. 4 The sorption degree (R , %) of anatase vs. duration of sorption time

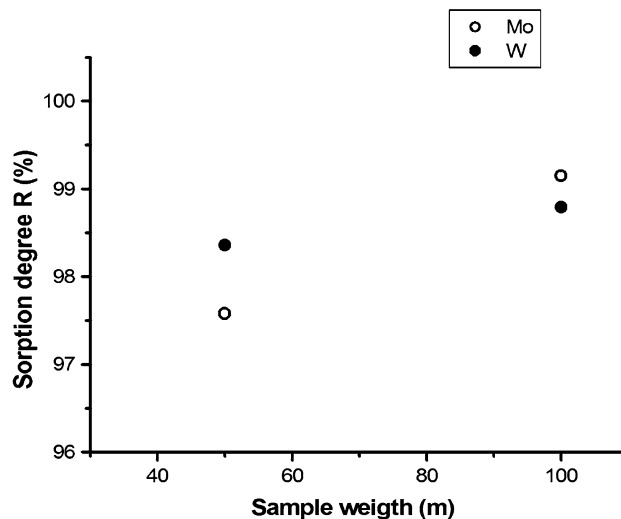


Fig. 5 The sorption degree (R , %) of Hombikat UV100 vs. sample weight

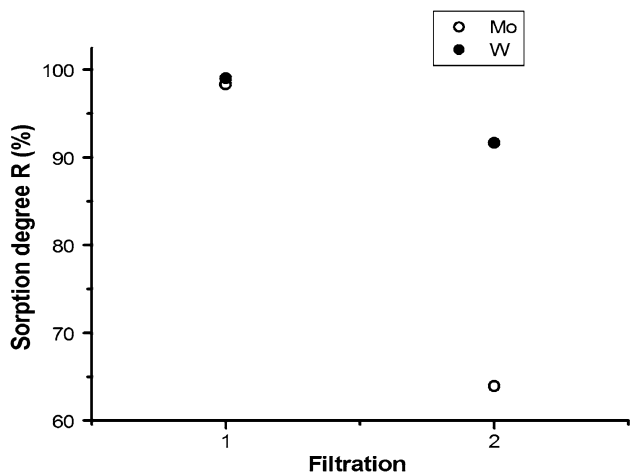


Fig. 6 The sorption degree (*R*, %) of anatase with 1 and without 2 filtration through a membrane filter

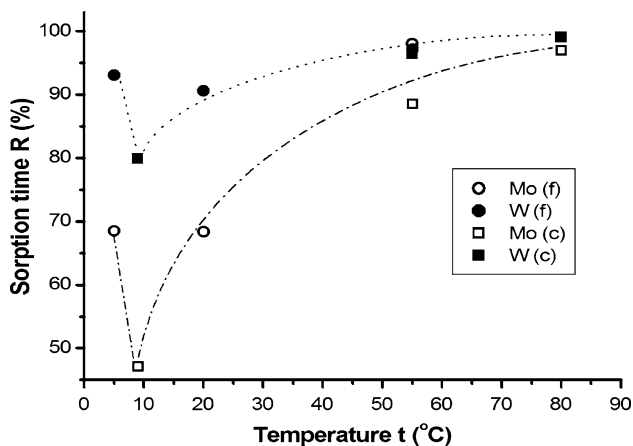
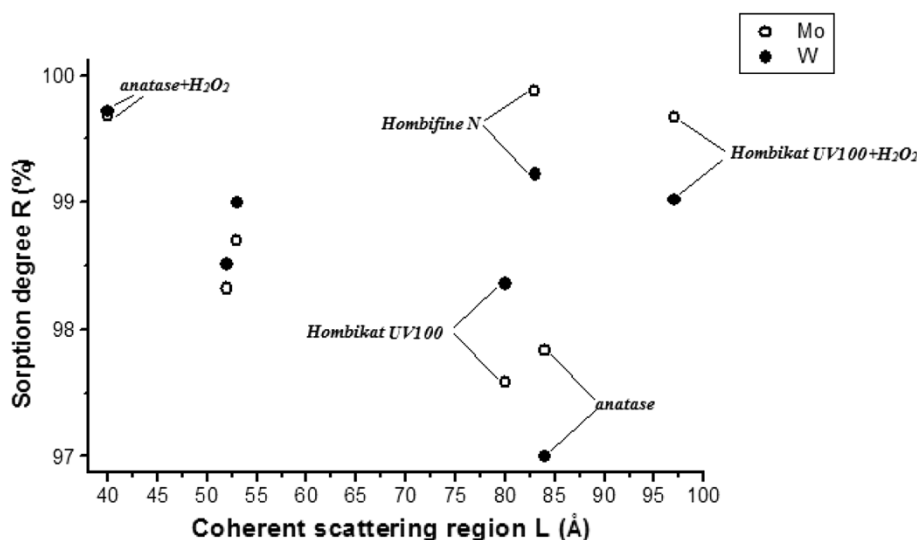


Fig. 7 The sorption degree (*R*, %) of anatase vs. sorption temperature: *f* filtration through a membrane filter, *c* centrifugation during 1 min

Fig. 8 The sorption degree (*R*, %) of studied samples with anatase vs. the coherent scattering region size (*L* value)



a negative charge (a similar to As(V) and Mo(VI) ions (Valencia-Trejo et al. 2010; Deedar et al. 2009; Xiao et al. 2007; Von Tytko et al. 1983). At low temperatures, they are adsorbed at the expense of forces of electrostatic character.

With temperature increasing from 4 to 10 °C, the attractive forces between TiO₂ and analytes are weakened and the adsorption decreases. Besides, at increasing temperature, the thickness of the boundary layer decreases due to the increasing tendency of the adsorbate to escape from the surface of the adsorbent to the solution phase, which results in a decrease in adsorption as previously reported by Igwe and Abia (2007).

It was found that in the temperature range from 10 to 85 °C the process is endothermic, since the adsorption increases with increasing temperature (Fig. 7). Therefore, the rate of physical adsorption and the amount of ions adsorbed by this way decrease, meanwhile the degree of chemical adsorption increases.

The increase in the sample dispersity under their grinding can result in either increase [for Mo(VI)] or decrease [for W(VI)] of the sorption degree.

Correlations between the sorption degree and sample characteristics are less obvious, since it is difficult to choose samples differing by only one parameter. However, in some cases (for our standard sorption conditions, *t* = 20 °C, *T_S* = 21 h, *m* = 50 mg, pH 0.35), the sorption degree was found to correlate with the samples characteristics (*N*, *S*, *V_U*, *V_N*). Particularly, these experimental relationships for Hombifine N and Degussa P25 and our samples with nanosized anatase (Table) can be described by equations (close to *R_{max}*):

$$R(N) = -23.44 \times 10^{-4}(N - 1.3346)^2 + 0.0875(N - 1.3346) + 99.1852(R_{\max} \text{ for } N_{SEM,CM} \sim 20 \text{ nm});$$

$$R(S) = -1.62 \times 10^{-4}(S + 7.2302)^2 + 0.0292(S + 7.2302) + 98.6778(R_{\max} \text{ for } S_{\text{CM}} \sim 83 \text{ m}^2/\text{g});$$

$$R(V_U) = -574.9033(V_U)^2 + 52.4378(V_U) + 98.7976(R_{\max} \text{ for } V_U = 0.046 \text{ cm}^3/\text{g});$$

$$R(V_N) = -79.1667(V_N)^2 + 38.391(V_N) + 95.3455(R_{\max} \text{ for } V_N = 0.242 \text{ cm}^3/\text{g}) \text{ (for W);}$$

$$R(N) = -20.10 \times 10^{-4}(N + 2.4932)^2 + 0.0666(N + 2.4932) + 99.4433(R_{\max} \text{ for } N_{\text{SEM,CM}} \sim 14 \text{ nm});$$

$$R(S) = -15.9 \times 10^{-4}(S + 0.1481)^2 + 0.3421(S + 0.1481) + 81.5713(R_{\max} \text{ for } N_{\text{SEM,CM}} \sim 14 \text{ nm})$$

$$R(V_U) = -129.845(V_U)^2 + 14.347(V_U) + 99.604(R_{\max} \text{ for } V_U = 0.055 \text{ cm}^3/\text{g});$$

$$R(V_N) = -19.217(V_N)^2 + 10.280(V_N) + 98.625(R_{\max} \text{ for } V_N = 0.267 \text{ cm}^3/\text{g}) \text{ (for Mo)}.$$

Anatase modified with H_2O_2 has the smallest value of the coherent scattering region size ($L = 40 \text{ \AA}$) and the highest (comparing to other samples, excluding Degussa P25) sorption degree of W(VI) (Fig. 8; Table 1). Similar results were obtained earlier for As(III), As(V), Bi(V) and V(V) (Dadachov 2006a, b; Meng et al. 2003; Valencia-Trejo et al. 2010; Deedar et al. 2009).

However, there is no correlation between the coherent scattering region size L (\AA) and the sorption degree (R , %). The maximal recovery efficiency from aqueous solutions of Mo(VI) ions has been obtained for Hombifine N with $L = 83 \text{ \AA}$ and Degussa P25 with $L = 250 \text{ \AA}$ (Fig. 10; Table 1). Hombikat UV100 has characteristics similar to Hombifine N (Table 1) except the specific surface area and composition of the sample. Nevertheless, Hombikat UV100 showed the worse adsorption ability as compared to Hombifine N (Fig. 10). The results led to the conclusion that the maximal recovery efficiency depends on concentration of adsorption centers—OH groups—on the adsorbent surface (Dadachov 2006a, b). Indeed, although the specific surface area of Hombikat UV100 is higher than for Hombifine N because of the presence of hydrous amorphous titanium dioxide (Fig. 2b), the concentration of OH groups on the surface of Hombikat UV100 is lower. Only the sample containing pure hydrous amorphous titanium dioxide has the characteristics ($S_{\text{BET}} = 317.5 \text{ m}^2/\text{g}$ and $S_{\text{C}} = 46.0 \text{ m}^2/\text{g}$, $V_U = 0.099 \text{ cm}^3/\text{g}$ and $V_N = 0.229 \text{ cm}^3/\text{g}$) and sorption degree ($R_{\text{Mo}} = 91.70 \%$ and $R_{\text{W}} = 97.72 \%$) that are lower than for Hombikat UV100 with $R_{\text{Mo}} = 97.50 \%$ and $R_{\text{W}} = 98.40 \%$. However, Hombikat UV100 modified with H_2O_2 by the cold

impregnation (Fig. 2c) shows the sorption degree ($R_{\text{Mo}} = 99.70 \%$ and $R_{\text{W}} = 99.05 \%$) second to Degussa P25 and the highest (among another samples, excluding Degussa P25) L value (Figs. 8, 10; Table 1). So, the treatment of the reaction mixture with hydrogen peroxide led decrease of the L value for anatase in contrast to the cold impregnation that increases this value (Table 1). Our experience suggests that the additional treatment of samples with hydrogen peroxide is of particular value for the

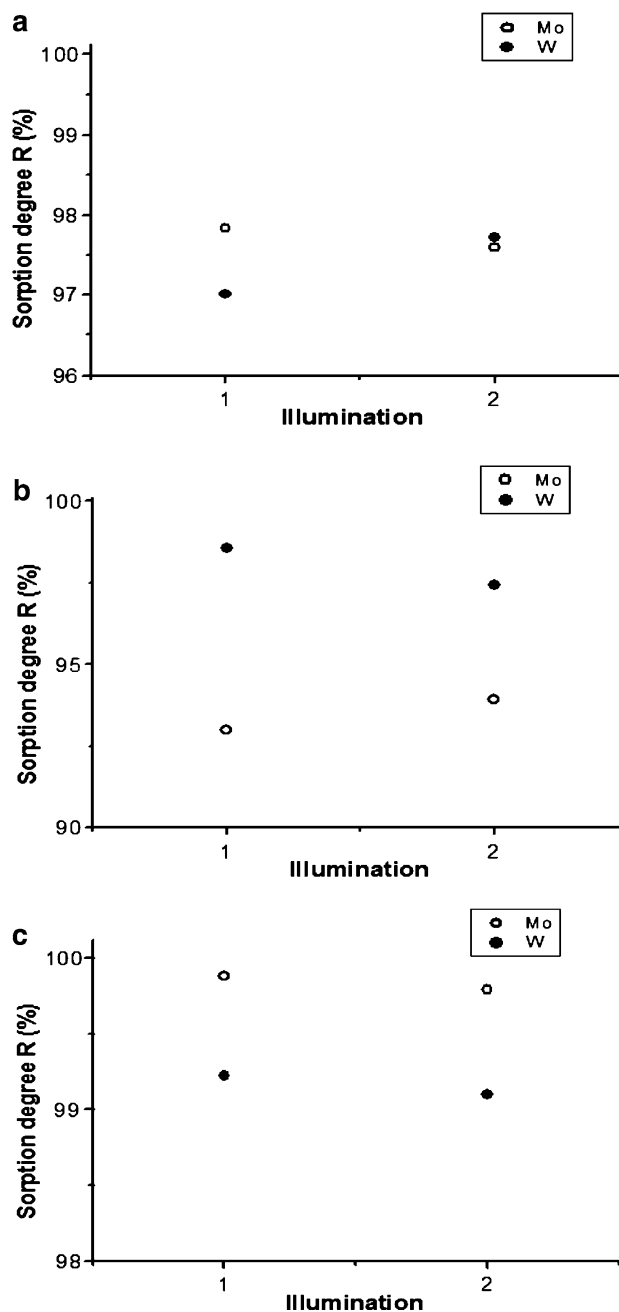
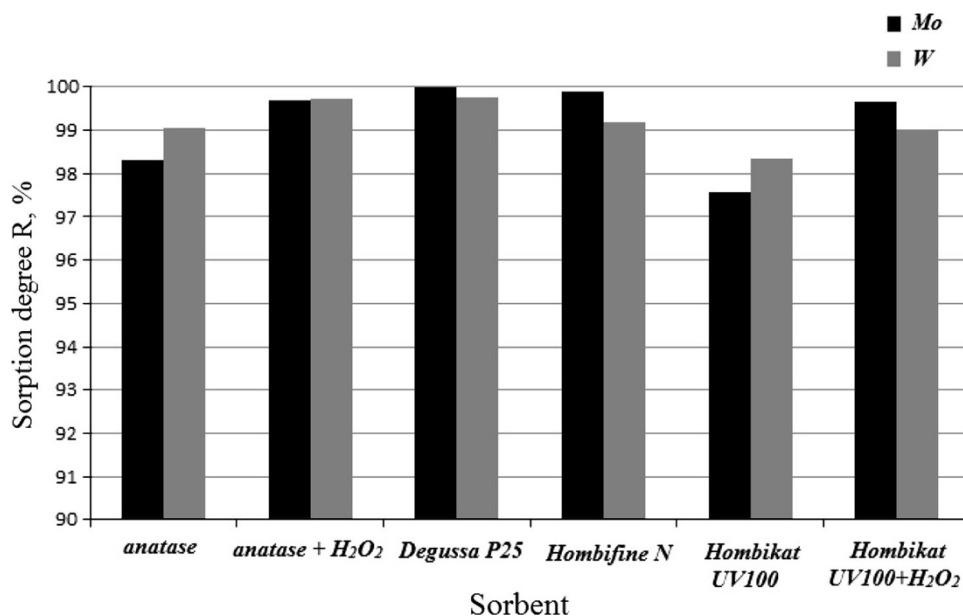


Fig. 9 The sorption degree (R , %) with 1 and without 2 illumination for different sorbents: anatase (a), Degussa P25 (b), Hombifine N (c)

Fig. 10 The sorption degree (R) vs. kinds of adsorbents and analytes



increase in the sorption degree associated with appearance of the O–O–H groups on the surface of particles.

On the other hand, nature of analytes affects the sorption degree. The nanoparticle surface of the studied samples contains cracks and pores of different scales which more or less deeply penetrate into the adsorbent. Their existence, especially ultrananopores, which size is comparable with a size of ions ($R_{\text{Mo}} = 0.69 \text{ \AA}$, $R_{\text{W}} = 0.60 \text{ \AA}$; ionic radius), considerably complicates the adsorption process. Large ions cannot penetrate into ultrananoporous of small sizes due to steric reasons; therefore, the ultraporous adsorbent possesses lower specific surface for such ions, as compared to smaller adsorbed ions.

The observed correlations between the R value and the sample illumination depend on the kind of analytes and the characteristics of adsorbents (specific surface area, volume of nano- and ultrananopores, nanoparticles and coherent scattering region sizes) (Fig. 9).

We have reached the maximal recovery efficiency of Mo(VI) ions sorption from aqueous solutions for the sample of commercial Hombifine N ($R = 99.90 \%$; sorption conditions with the use of a membrane filter with $0.45 \mu\text{m}$ pores: $t = 20 \text{ }^\circ\text{C}$, $T_{\text{S}} = 21 \text{ h}$, $m = 50 \text{ mg}$), of Mo(VI) and W(VI) ions sorption for the sample of commercial Degussa P25 ($R_{\text{Mo}} = 99.99 \%$ and $R_{\text{W}} = 99.75 \%$; sorption conditions with the use of centrifugation during 1 min: $t = 80 \text{ }^\circ\text{C}$, $T_{\text{S}} = 3 \text{ h}$, $m = 50 \text{ mg}$) and for nanosized anatase modified with H₂O₂ ($R = 99.75 \%$; standard sorption conditions with the use of a membrane filter with $0.45 \mu\text{m}$ pores) (Fig. 10).

In general, the obtained experimental data show the role of sorption conditions, sorbent characteristics and analyte

nature in the process of Mo(VI) and W(VI) extraction from aqueous solutions.

Conclusions

The adsorption of Mo(VI) and W(VI) ions in the form of associates of different nature on Degussa P25, Hombifine N, Hombikat UV100 and the synthesized samples with the anatase structure significantly depends on temperature, decrease in the $4\text{--}10 \text{ }^\circ\text{C}$ range and increase in the $10\text{--}85 \text{ }^\circ\text{C}$ range. This behavior indicates an exothermic and endothermic nature of the adsorption process in the given ranges, respectively. In addition, the sorption degree of Mo(VI) and W(VI) ions adsorption depends on the contact duration, sample weight, and kind treatment. The higher sorption degree correlates to the formation of the O–O–H groups on treatment of the samples with hydrogen peroxide.

As a result, we have found that all the samples with nano-sized anatase show high adsorption ability for Mo(VI) and W(VI) ions with $R \geq 99.75 \%$. The similar properties were earlier obtained for As(III,V), Bi(V), V(V) (Kuzmicheva et al. 2012) and can be found for other ions. Due to its unique adsorption properties, nanosized anatase is a promising material for extraction of various ions from aqueous solutions.

Acknowledgments Authors would like to acknowledge financial support from Federal Targeted Programme (FTP) “Scientific and Scientific-Pedagogical Personnel of the Innovative Russia” (2012–2013) for supporting this work through the Grant No. 14.B37.21.1621.

Open Access This article is distributed under the terms of the Creative Commons Attribution License which permits any use, distribution, and reproduction in any medium, provided the original author(s) and the source are credited.

References

- Bleam WF, McBride MB (1986) The chemistry of adsorbed Cu(II) and Mn(II) in aqueous titanium dioxide. *J Colloid Interface Sci* 110:336–346
- Brunauer S, Emmett PH, Teller E (1938) Adsorption of gases in multimolecular layers. *J Am Chem Soc* 60:309–319
- Dadachov M (2006) Novel titanium dioxide, process of making and method of using same. US Pat. Appl. 0171877, 3 Aug 2006
- Dadachov M (2006) Novel adsorbents and process of making and using same. US Pat. Appl. 0144793, 6 July 2006
- Deedar N, Irfan A, Ishtiaq Q (2009) Evaluation of the adsorption potential of titanium dioxide nanoparticles for arsenic removal. *J Environ Sci* 21:402–408
- Dzis'ko VA, Karnaukhov AP, Tarasova DV (1978) Physicochemical principles of oxide catalyst synthesis. Nauka, Novosibirsk (in Russian)
- Gao Y, Wahi R, Kan AT, Falkner JC, Colvin VL, Tomson MB (2004) Adsorption of cadmium on anatase nanoparticles effect of crystal size and pH. *Langmuir* 20:9585–9593
- Georgaka A, Spanos N (2010) Study of the Cu(II) removal from aqueous solutions. *Glob NEST J* 12:239–247
- Gregg S, Sing K (1982) Adsorption, surface area, and porosity. Academic Press, New York
- Igwe JC, Abia AA (2007) Studies on the effects of temperature and particle size on bioremediation of As(III) from aqueous solution using modified and unmodified coconut fiber. *Glob J Environ Res* 1:22–26
- Kuzmicheva GM, Savinkina EV, Obolenskaya LN, Belogorokhova LI, Mavrin BN, Chernobrovkin MG, Belogorokhov AI (2010) Preparation, characterization and properties of nano-sized titanium dioxide modifications with the structures of anatase and η -TiO₂. *Cryst Rep* 55:866–871
- Kuzmicheva GM, Natykan AA, Savinkina EV, Obolenskaya LN, Domoroshchina EN, Yakovenko AG (2012) A way of preparing adsorbent on the basis of nanosized titanium dioxide with anatase structure. RU Patent 2,463,252, 10 Oct 2012
- Meng X, Dadachov M, Korfiatis GP, Christodoulatos C (2003) Methods of preparing a surface-activated and using same in water treatment processes. US Pat. Appl. 0155302, 23 August 2003
- Obolenskaya LN, Kuzmicheva GM, Savinkina EV, Zhilkina AV, Sadovskaya NV, Prokudina NA, Chernyshev VV (2012) Influence of conditions of a sulphatic method on characteristics of samples with nanosized modification of anatase. *Her RAS Chem* 11:2032–2038
- Savinkina EV, Kuz'micheva GM, Tabachkova NYu, Obolenskaya LN, Demina PA, Yakovenko AG (2011a) Synthesis and morphology of anatase and η -TiO₂ nanoparticles. *Inorg Mater* 47:489–494
- Savinkina EV, Kuzmicheva GM, Obolenskaya LN (2011b) Efficient synthesis and properties of η -titania. 2nd European Conference of Chemical Engineering, Puerto De La Cruz
- Svergun DI (1992) Determination of the regularization parameter in indirect-transform methods using perceptual criteria. *J Appl Crystallogr* 25:495–503
- Tella T, Panagiotou GD, Petsi T, Bouriras K, Kordulis C, Lycourghiotis A (2010) The mechanism of retention of vanadium oxo-species at the “titanium oxide/aqueous solution” interface. *Glob NEST J* 12:231–238
- Valencia-Trejo E, Villicaña-Méndez M, Alfaro-Cuevas-Villanueva R, Garnica-Romo MG, Cortés-Martínez R (2010) Effect of Temperature on the Removal of Arsenate from Aqueous Solutions by Titanium Dioxide Nanoparticles. *J Appl Sci Environ Sanit* 5:171–184
- Von Tytko KH, Baethe G, Hirschfeld ER, Mehmke K, Stellhorn D (1983) Über die Gleichgewichte in wäßrigen Polymolybdatlösungen Neuauswertung der potentiometrischen Meßdaten von Sasaki und Sillen. *Z Anorg Allg Chem* 5080:43–66
- Xiao Y, Ling J, Qian Sh, Lin A, Zheng W, Xu W, Luo Yu, Zhang M (2007) Preconcentration of trace arsenite and arsenate with titanium dioxide nanoparticles and subsequent determination. *Water Environ Res* 79:1015–1022
- Zagrafskaya RV, Karnaukhov AP, Felonov VB (1975) The globular model of porous bodies with corpuscular structure. III Study of random and partially ordered packed spheres. *Kinet Catal* 16:1583–1590
- Zhilkina AV, Gordienko AA, Prokudina NA, Trusov LI, Kuz'micheva GM, Dulina NA, Savinkina EV (2013) Determination of the size of particles of highly dispersed materials by low temperature nitrogen adsorption. *Russ J Phys Chem A* 87:674–679